Journal of Manufacturing Processes 68 (2021) 1849–1859

Contents lists available at ScienceDirect

Journal of Manufacturing Processes

journal homepage: www.elsevier.com/locate/manpro

Bead shape control in wire based plasma arc and laser hybrid additive manufacture of Ti-6Al-4V

Chong Wang *, Wojciech Suder, Jialuo Ding, Stewart Williams

Welding Engineering and Laser Processing Centre, Cranfield University, Cranfield, Bedfordshire MK43 0AL, UK

ARTICLE INFO

Keywords:
Wire based additive manufacture
PTA-laser hybrid additive manufacture
Bead shape
Titanium

ABSTRACT

Wire based plasma transferred arc (PTA)-laser hybrid additive manufacture has the potential to build large-scale metal components with high deposition rate and near-net shape. In this process, a single bead is the fundamental building block of each deposited component, and thus the bead shape control is essential for the deposition of different geometries. However, how to control the bead shape by manipulating various process parameters is still not understood. In this study, the effect of different process parameters, including laser power, energy distribution between the PTA and laser, wire feed speed, travel speed, and laser beam size on the deposition process and bead shape was investigated systematically. The results show that the optimum operating regime for the hybrid process is with the wire being fully melted by the PTA and the melt pool being controlled by the laser, which gives a good bead shape as well as a stable deposition process. The bead shape is significantly affected by the laser power and travel speed due to the large variation in energy input. The effect of wire feed speed is more complex with the bead width initially increasing to a maximum and then decreasing as the wire feed speed increases. The laser beam size has a minor effect on the bead shape, but a small beam size will result in an irregular bead appearance due to the unstable process caused by the high power density. In addition, a procedure for controlling the bead shape in the hybrid process was proposed, which provided a reference for selection of different process parameters to achieve required bead shapes. The feasibility of this proposed procedure was demonstrated by the two deposited multi-layer single-pass walls.

1. Introduction

Compared to traditional subtractive and formative manufacture methods, additive manufacture (AM) is attracting more attention due to the massive reduction of wasted material, relatively short lead-time, no mould and die needed, and high design flexibility [1–3]. In metal AM, powder or wire is commonly used as a feedstock, melted by a heat source of laser, electron beam or electric arc. Amongst different AM techniques, wire + arc additive manufacture (WAAM) is most cost-effective due to lower cost of wire compared to powder and higher efficiency of electric arc compared to laser and electron beam, and therefore is suitable for deposition of large structural components with high deposition rate [4–7]. In plasma transferred arc (PTA) based WAAM, typical deposition rates of titanium are 0.4–1.2 kg/h. Much higher deposition rates can be achieved (e.g., Norsk Titanium [8]) but at the cost of low surface quality, resulting in significant material needing to be machined off. Wire based PTA-laser hybrid AM has shown the potential to build large-scale components with both high deposition rate and near-net shape [9]. It combines the advantages of both heat sources (i.e., high efficiency of the PTA and high precision of the laser) and shows more benefits than PTA or laser deposition processes on their own. For example, the hybrid deposition process has lower likelihood of keyhole formation than the PTA deposition process, and higher deposition rate and process tolerance than the laser deposition process. In addition, it allows independent control of deposition rate and bead shape, which is difficult to accomplish with a single heat source. During the deposition process, a single bead is the smallest and fundamental unit, which determines the final surface quality and dimensional accuracy of a deposited part. Therefore, it is critical to understand how individual process parameters affect the bead shape and how to achieve targeted bead dimensions in order to achieve a reliable process for deposition of a wide range of geometries.

Wire based arc-laser hybrid AM process has not been studied widely. So far, most of the parametric studies on bead shape using arc-laser hybrid heat sources are focused on welding applications [10–13]. However, in hybrid welding, the laser beam is generally used for its deep penetration capability, and hence the laser is operated with small beam

* Corresponding author.
E-mail address: chong.wang1@cranfield.ac.uk (C. Wang).

https://doi.org/10.1016/j.jmapro.2021.07.009
Received 10 April 2021; Received in revised form 15 June 2021; Accepted 4 July 2021
Available online 16 July 2021

size in the keyhole regime [14]. In hybrid AM, however, the laser is used to provide additional energy and support the arc in melting the wire and spread the melt pool. Therefore, conduction regime is more appropriate in hybrid AM process. In addition, in a large number of hybrid welding cases, a much lower volume of filler wire is required compared to that in an AM process. Therefore, the different practical requirements between welding and AM lead to different optimum working conditions, meaning that the results obtained in a hybrid welding process might not be applicable to a hybrid AM process. To the best knowledge of the authors, no systematic study about bead shape control in arc-laser hybrid AM has been reported.

There has been a lot of effort dedicated to developing such process understanding in wire based arc or laser AM processes. Dinovitzer et al. [15] used a Taguchi method to study the effect of different process parameters, including wire feed speed (WFS), travel speed (TS), and current, on the bead geometry in gas tungsten arc (GTA) deposition process. They concluded that the bead width decreased whilst the bead height increased with the increase of WFS. The TS had a major effect on bead width but a minor effect on bead height. In addition, the bead width increased with increasing current. Such process understanding is required to develop process algorithms for the deposition of engineering parts. However, the selected process window was quite narrow (e.g., current ranging only from 50 to 59 A) in their study. Martina et al. [16] investigated the PTA deposition of titanium for a much wider range of parameters (e.g., current ranging from 120 to 300 A). They found that the effective wall width increased with increasing current and decreasing TS, and the layer height increased with increasing WFS and decreasing current. In addition to arc based deposition processes, bead shape control in laser wire deposition process was also studied. Schulz et al. [17] achieved process maps using a semi-analytical approach to study the bead width as a function of WFS, laser power, and laser intensity distribution in laser wire deposition process and achieved similar results as described in arc based processes in Refs. [15,16]. In addition, they reported that the process was sensitive to the ratio of WFS to TS, where a low ratio led to the formation of droplets and process instabilities. Abioye et al. [18] developed a process map to predict the process characteristics and bead geometry in laser wire deposition process and achieved the relationship between the input parameters (WFS, TS, and laser power) and the resulting bead properties (contact angle, width-height aspect ratio, and dilution ratio). Mok et al. [19] studied the influence of laser power, TS, and WFS on the bead shape, and claimed that the bead width was mainly determined by laser power whilst the bead height was affected more significantly by TS than by laser power.

Similar work needs to be done for the wire based PTA-laser hybrid AM process to achieve desired bead shapes for the deposition of complex components. It is known that WFS and TS are two of the most critical process parameters that need to be considered to control the bead shape. In addition, the energy is provided by both the PTA and laser in the hybrid AM process, which contribute to the melting of wire and spread of melt pool. Therefore, the influence of both heat sources needs to be considered. Nevertheless, there are different operating ranges for the two heat sources. For example, in the PTA deposition process, a keyhole can be formed at high current levels caused by high arc pressure, which can result in defect formation [20], whilst excessive power density in a laser based process can lead to vaporisation and melt pool instabilities [9]. Therefore, in the PTA-laser hybrid deposition process, for a given total power input the process stability and the bead shape will vary depending on the ratio of arc power to laser power. However, how these parameters affect the deposition process and the bead shape is not understood. Also, a procedure for selecting different process parameters needs to be developed to provide references for controlling the bead shape in the hybrid process.

In this study, the effect of different process variables, including laser power, the ratio of arc power to laser power, WFS, TS, and laser beam size, on the bead shape formation in wire based PTA-laser hybrid AM process of Ti-6Al-4V was studied systematically. The goal was to understand the effect of each process parameters on the deposition process and bead shape, and develop a procedure for the selection of process parameters to achieve a targeted bead shape in the hybrid deposition process.

2. Experimental procedure

2.1. Materials and setup

The material used for substrate and wire was Ti-6Al-4V. The diameter of the wire was 1.2 mm, and the dimensions of the substrate were 300 mm × 200 mm × 7 mm. Before deposition, the substrate was first ground and then cleaned with acetone to remove any surface contamination. Fig. 1 shows the experimental setup for the wire based PTA-laser hybrid AM system. The PTA was generated by a EWM Tetrix 552 power supply. Pure argon was used for both shielding gas (flowrate: 8 L/min) and plasma gas (flowrate: 0.8 L/min) for the plasma torch. An AMV 4000 arc monitor was connected to the plasma arc power supply to recorder the arc voltage and arc current. An IPG fibre laser with a wavelength of 1070 nm and a maximum power of 8 kW was used. The laser beam used in this study was defocused (i.e., out of the focal position, see Fig. 2). The laser head was inclined at an angle of 30° to prevent back reflection. The wire was fed using a Dinse wire feeder. A 6-axis Fanuc robot with mounted plasma torch and laser head was used to control the deposition path. The experiments were conducted in a flexible transparent enclosure (tent) purged with pure argon. During the deposition, the oxygen level in the enclosure was controlled to be below 500 ppm as verified by a PurgEye 600 oxygen analyser. A CMOS process camera (Xiris XVC-1000) was fixed perpendicular to the travel direction to monitor the melt pool behaviour and metal transfer process.

Fig. 2 schematically shows the configuration used in this study, which is the optimum operating condition for the PTA-laser hybrid AM process according to Ref. [9], allowing high process tolerance and high deposition rate. In this configuration, the wire was irradiated by the PTA and the laser was placed behind the PTA. The plasma torch was positioned with a stand-off distance of 8 mm and inclination angle of 20° to ensure enough access for the wire and avoid laser reflection. The wire feeding angle was 15°. The distance (d_1) between the wire tip and the substrate was 2 mm, whilst the separation distance (d_2) between the PTA and the laser was 10 mm. It should be mentioned that this wire feeding position is in the optimum range of the hybrid deposition process, which gives stable deposition process and uniform bead shape [9].

2.2. Methods

The bead shape was characterised by three features, which are bead width, bead height, and contact angle (θ), as illustrated in Fig. 3. It is worth mentioning that the contact angle determines the wetting and spreading of the deposited material. For wire based AM processes, lower contact angle means better wettability of the material, leading to lower surface waviness. Prior to the parametric study, preliminary trials were conducted to find out the appropriate range for different process parameters. After that, in the first experiment, the effect of laser power on bead shape was investigated. The laser power was increased from 1 to 7 kW with an increment of 2 kW at constant other conditions, as shown in Table 1 (Cases 2–5). In addition, a deposit just with PTA and without any laser was conducted as a reference (Case 1, Table 1).

In the next experiment, the effect of the ratio of arc power to laser power on the bead shape was investigated (Cases 6–11, Table 1). The laser power was increased from 0 to 5 kW, whilst the arc power was reduced from 8 to 3 kW, maintaining the total power input constant at 8 kW. The output power of the PTA was calculated based on applied voltage and current, measured by the arc monitor. To study the effect of WFS on bead shape, the WFS was increased from 2 to 6 m/min with an increment of 1 m/min (Cases 12–16, Table 1). Also, to study the effect of

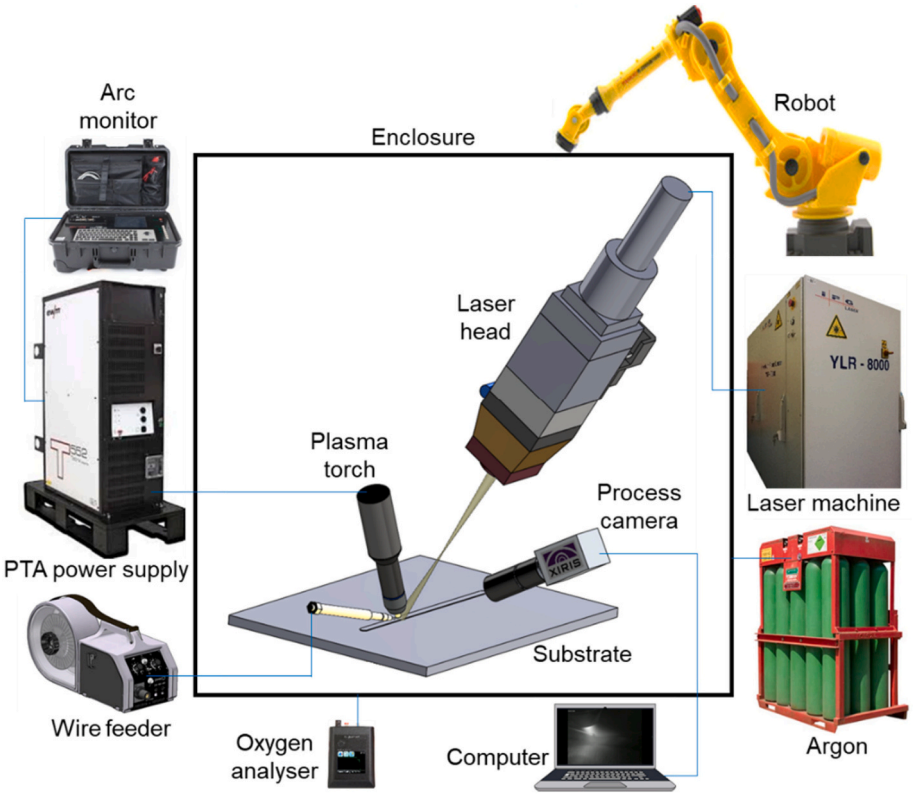

Fig. 1. Experimental setup for the wire based PTA-laser hybrid AM process.

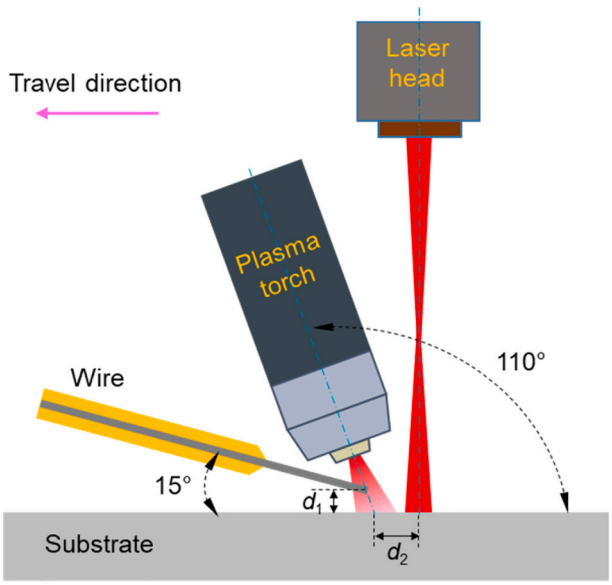

Fig. 2. Configuration used for the wire based PTA-laser hybrid AM process (side view).

TS on bead shape, the TS was increased from 4 to 12 mm/s with an increment of 2 mm/s by keeping other parameters fixed (Cases 17–21, Table 1).

To study the effect of laser beam size on bead shape, the laser beam diameter was increased from 2 to 12 mm with an increment of 2 mm (Cases 22–27, Table 1). In addition, some deposits with different laser beam diameters (5, 12, and 15.6 mm) were conducted at different laser powers.

In addition, two multi-layer single-pass walls with the same bead shape but different deposition rates were deposited to prove that the bead shape in the hybrid process can be controlled according to a proposed procedure.

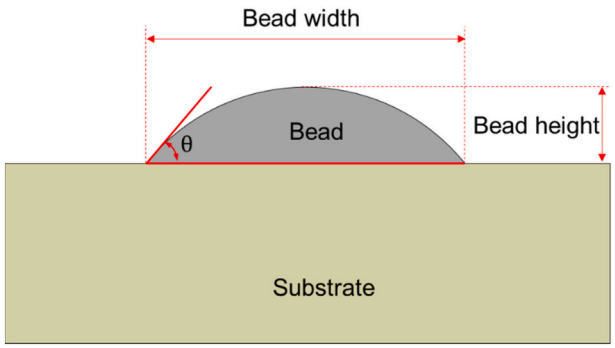

Fig. 3. Schematic diagram of the cross-section showing the bead width, bead height, and contact angle (θ).

After deposition, some beads and the two single-pass walls were cross-sectioned, hot mounted, ground, polished, and etched in Kroll's reagent and their properties (e.g., profile and remelting region) were observed using stereomicroscopy. All the beads had a same length of 120 mm, and the bead dimensions were measured at the length of 30 mm, 60 mm, and 90 mm from the initiation, and an average value was used. It should be mentioned that the contact angle was measured on both sides of the beads using the software AxioVision.

Table 1
Process parameters used to study the effect of each parameters on the bead shape.

Parametric study	Case	Arc current (A)	Arc power (kW)	Laser power (kW)	WFS (m/min)	TS (mm/s)	Laser beam diameter (mm)
Laser power	1	200	4.8	0	4	4.5	12
	2	200	4.8	1	4	4.5	12
	3	200	4.8	3	4	4.5	12
	4	200	4.8	5	4	4.5	12
	5	200	4.8	7	4	4.5	12
Ratio of arc power to laser power	6	276	8	0	4	4.5	12
	7	254	7	1	4	4.5	12
	8	230	6	2	4	4.5	12
	9	205	5	3	4	4.5	12
	10	176	4	4	4	4.5	12
	11	143	3	5	4	4.5	12
WFS	12	200	4.8	3	2	4.5	12
	13	200	4.8	3	3	4.5	12
	14	200	4.8	3	4	4.5	12
	15	200	4.8	3	5	4.5	12
	16	200	4.8	3	6	4.5	12
TS	17	200	4.8	5	4	4	12
	18	200	4.8	5	4	6	12
	19	200	4.8	5	4	8	12
	20	200	4.8	5	4	10	12
	21	200	4.8	5	4	12	12
Laser beam size	22	200	4.8	5	4	4.5	2
	23	200	4.8	5	4	4.5	4
	24	200	4.8	5	4	4.5	6
	25	200	4.8	5	4	4.5	8
	26	200	4.8	5	4	4.5	10
	27	200	4.8	5	4	4.5	12

3. Results and discussion

3.1. Different process parameters on bead shape

3.1.1. Effect of laser power

Fig. 4 shows the deposition process and the resulting cross-sections of the beads obtained with different laser powers. The corresponding bead dimensions (width and height) and contact angle are plotted in Fig. 5. It can be seen that initially the bead was narrow and tall with only PTA (i.e., laser power of 0 kW). The bead shape did not change significantly (bead width increased only from 7.23 to 7.45 mm) with an extra 1 kW laser power, suggesting this laser power was not high enough to expand the melt pool in the transverse direction. It is worth mentioning that because this WFS was relatively high, close to the limit for this current, the first two macrographs exhibit low remelting into the substrate, as almost the entire arc power was utilised for melting the wire. When the laser power was increased from 1 to 3 kW, the melt pool became much wider and shallower, leading to a sudden increase in bead width and decrease in bead height (Fig. 5a). The melt pool became flatter remarkably with a further increase of laser power to 7 kW. As for the contact angle, it decreased constantly due to an increased width-height aspect ratio of the beads (Fig. 5b), indicating a better wettability of the material on the workpiece.

It also can be seen from Fig. 4b that the remelting into the substrate increases with the increase of laser power. In particular, at a laser power of 5 and 7 kW, the penetration depth was very high, as indicated by the heat-affected zone. This leads to remelting of several layers lying below the layer being deposited during the deposition process. Such a process will result in low deposition process efficiency and high distortion, as revealed in Ref. [9]. Therefore, in this case, a laser power of 3–5 kW is optimum, and then further increase will cause too much remelting.

3.1.2. Effect of the ratio of arc power to laser power

Fig. 6 shows the deposition processes with different ratios of arc power to laser power. It is known that in arc based processes the arc pressure increases with increasing arc current due to the increased electromagnetic force [20]. When the arc power (mainly controlled by current) was set to 8 kW, the high arc pressure caused a large depression in the melt pool (Fig. 6a). The depression became smaller and then disappeared as the arc power reduced, as shown in Fig. 6(b-e). However, when the arc power was too low (Fig. 6f), the wire could not be fully melted by the PTA and stabbed the melt pool, which induced oscillations in the melt pool. If the wire reaches the melt pool, it takes excessive heat from the melt pool, reducing the melting efficiency and in extreme cases leading to misalignment of the wire [9,20].

Fig. 7 shows the dimensions and contact angle of the beads obtained with the processes as presented in Fig. 6. The bead becomes wider and shallower as the ratio of arc power to laser power reduces. This is because the reducing arc power and increasing laser power cause less depression in the melt pool, which changes the energy source profile, leading to a change in bead shape. When the arc power is high, the high depression results in a three-dimensional energy source profile with relatively low energy at the surface, leading to a narrow bead. As the arc power reduces and laser power increases, the depression reduces and finally disappears. Consequently, the energy source goes shallower and becomes a two-dimensional surface energy source. This results in more energy at the surface and leads to wider bead. To compensate for the increased bead width, the bead height decreases constantly according to the conservation of mass. Besides, there is a decrease in contact angle with the increase of arc power-laser power ratio, as shown in Fig. 7b.

With the same total energy input of 8 kW, there was large depression in the melt pool in the PTA process (Fig. 6a), meaning a lower likelihood of keyhole formation can be achieved with the hybrid process (Fig. 6b-6e). By varying the ratio of arc power to laser power, different bead shapes can be achieved with the hybrid process (Fig. 7), which is difficult to accomplish with the PTA process. These demonstrated the benefits of the hybrid process over the single PTA process.

It has been shown in the literature that the bead shape affects the surface quality of deposited parts. Wang et al. [20] described that at the same cross-sectional area, a flatter bead (i.e., lower contact angle) leads to a lower surface waviness. Although the bead becomes flatter with increasing laser power and decreasing arc power (Fig. 7), too low arc power, at a certain point, will lead to an unstable deposition process with wire stabbing the melt pool (Fig. 6f). Therefore, in the PTA-laser hybrid deposition process, it is desired that when the arc power is just enough to melt the wire and the laser power is adjusted to control the

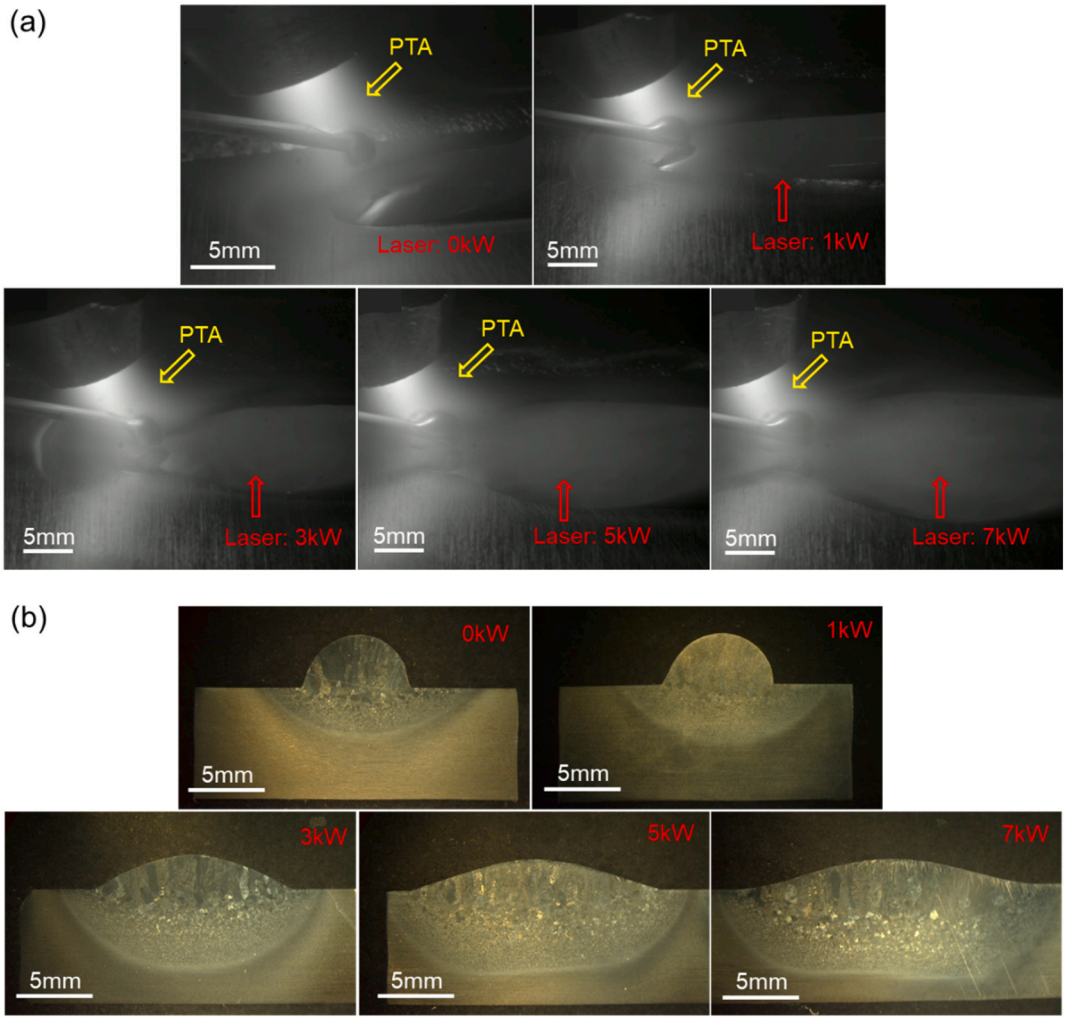

Fig. 4. The effect of laser power on (a) deposition process, and (b) bead shape at a constant arc power of 4.8 kW.

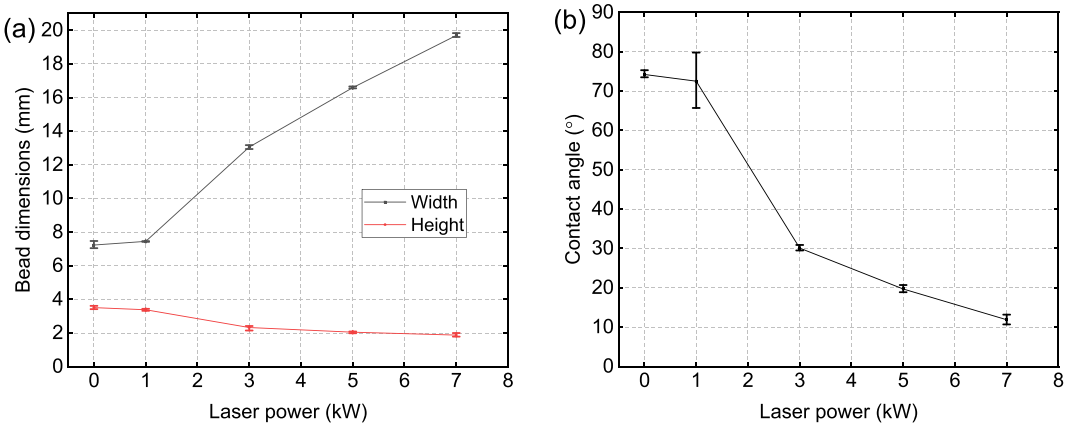

Fig. 5. The effect of laser power on (a) bead dimensions, and (b) contact angle. All the parameters used are shown in Cases (1–5) of Table 1.

melt pool width, but not too high thus to avoid excessive remelting into the underlying layers.

3.1.3. *Effect of wire feed speed*

Fig. 8 shows the deposition processes with different WFSs at an arc power of 4.8 kW (current of 200 A) and a laser power of 3 kW. When the WFS was low (2 m/min, Fig. 8a), the wire was fully melted even without reaching the centre of arc column. The arc pressure induced a depression in the exposed workpiece surface. As the WFS increased from 3 to 4 m/min (Fig. 8b and 8c), the wire could no longer be melted immediately at the edge of the arc column and started protruding to the opposite side, shielding the workpiece and dispersing the plasma force. Hence the depression gradually decreased and eventually disappeared at the WFS of 4 m/min. However, when the WFS reached 5–6 m/min, the wire could

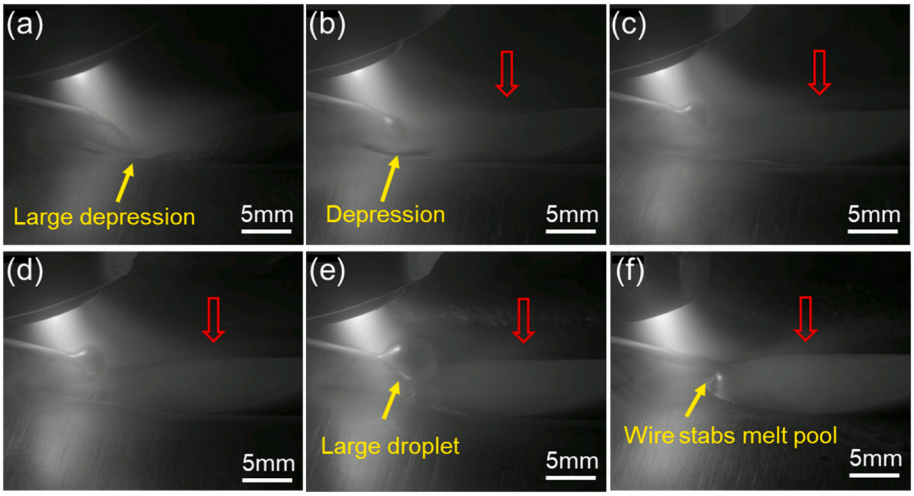

Fig. 6. The deposition processes with different ratios of arc power to laser power at a constant total applied power of 8 kW: (a) 8 kW arc, (b) 7 kW arc and 1 kW laser, (c) 6 kW arc and 2 kW laser, (d) 5 kW arc and 3 kW laser, (e) 4 kW arc and 4 kW laser, (f) 3 kW arc and 5 kW laser. Red arrows indicate the laser positions. (For interpretation of the references to colour in this figure legend, the reader is referred to the web version of this article.)

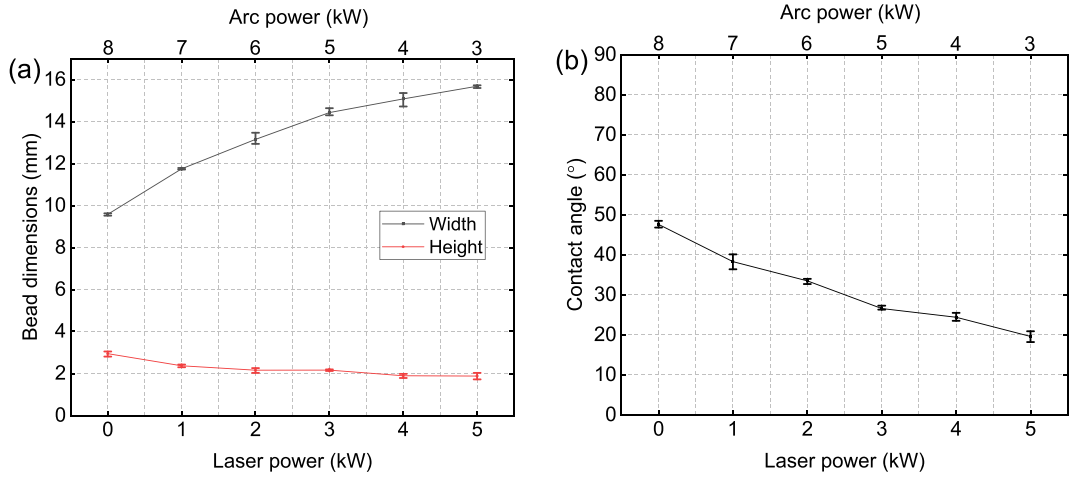

Fig. 7. The effect of the ratio of arc power to laser power on (a) bead dimensions, and (b) contact angle. All the parameters used are shown in Cases (6–11) of Table 1.

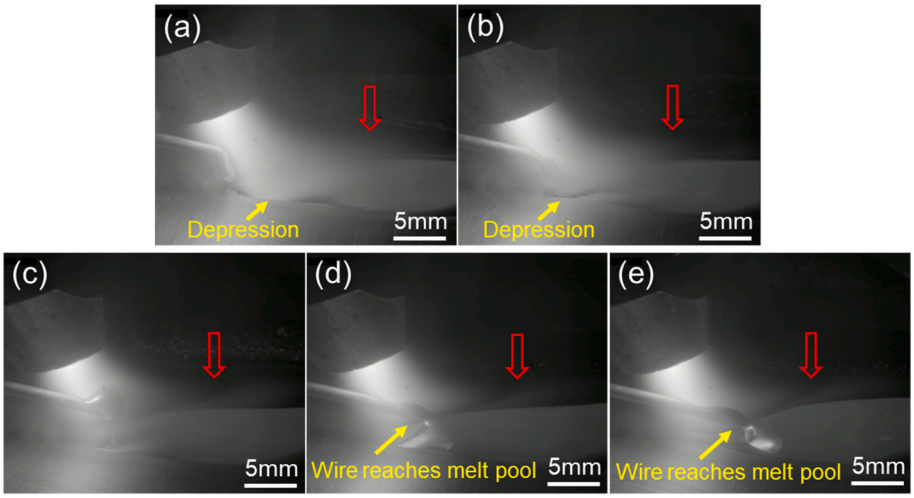

Fig. 8. The hybrid deposition processes at different WFSs: (a) 2 m/min, (b) 3 m/min, (c) 4 m/min, (d) 5 m/min, and (e) 6 m/min. Red arrows indicate the laser positions. (For interpretation of the references to colour in this figure legend, the reader is referred to the web version of this article.)

no longer be melted entirely by the PTA and reached the laser-generated melt pool (Fig. 8d and 8e).

Fig. 9 shows the bead dimensions and contact angle as a function of WFS. It can be seen that the bead width rises first and then declines as the WFS increases. A similar result was obtained in the PTA deposition process by Martina et al. [16]. However, the authors did not explain this phenomenon. Wang et al. [20] studied the effect of WFS on bead shape in the PTA deposition of Ti-6Al-4V, and also achieved a similar result. They stated that the increase of the bead width was attributed to the improved melting efficiency caused by lower thermal conduction of wire as compared to the workpiece. The reduction of bead width was attributed to the excessive heat taken from the melt pool by the wire. As for the bead height, it constantly increases due to the increased feeding rate. Also, the contact angle keeps increasing as the WFS increases, indicating a worse wetting of the workpiece.

It should be mentioned that the largest bead width was obtained at the WFS of 4 m/min, where the arc power is just enough to fully melt the wire (Fig. 8c). This confirms the conclusion obtained in Section 3.1.2 that in the PTA-laser hybrid AM process the arc power is optimum when it is just sufficient for melting the wire provided no significant depression is instigated in the melt pool. In general, there is a small effect of WFS on the bead width (8% variation, Fig. 9a), depending on whether the wire is melted directly by the PTA or it needs some extra heat from the laser-generated melt pool.

3.1.4. Effect of travel speed

Fig. 10 shows the deposition processes at different TSs. It can be seen that the wire could be fully melted by the PTA in all cases, meaning that the TS does not have a significant effect on wire melting behaviour. As described in Ref. [9], this configuration is best for the PTA-laser hybrid deposition process as the wire can be transferred into the melt pool smoothly by arc pressure and the process has high tolerance in terms of wire feeding space. Therefore, Fig. 10 demonstrates that such a configuration is insensitive to TS.

Fig. 11 shows the bead dimensions and contact angle obtained with the processes as presented in Fig. 10. It can be seen that both bead width and bead height decrease with the increase of TS (Fig. 11a). The heat input per unit length, Λ, is inversely proportional to the TS, which is given by:

$$\Lambda = \frac{P}{v_t} \tag{1}$$

where P is the total applied power, and v_t is TS. Therefore, increasing the TS reduces the heat input per unit length, leading to a reduction in bead width. During the deposition, if the material vaporisation and spatter are neglected, the material deposited per unit length (i.e., cross-sectional area of the bead), A_b, can be expressed by:

$$A_b = \frac{A_w v_w}{v_t} \tag{2}$$

where v_w is WFS, and A_w is the cross-sectional area of the wire. It can be seen that increase of TS leads to a decrease in material deposited per unit length. Therefore, both the bead width and bead height decrease with the increase of TS. In fact, the contact angle is determined by the width-height aspect ratio of the bead [18]. Although both bead width and height decrease with the increase of TS, the contact angle remains almost unchanged with a low value of 16°, as shown in Fig. 11b.

3.1.5. Effect of laser beam size

One of the biggest benefits of laser is independent control of beam size and power, which allows the power density and beam size to be independently varied. Fig. 12 shows the bead width as a function of laser beam diameter in the PTA-laser hybrid deposition process. It can be seen that the same bead width of 16.9 mm was obtained with the laser beam diameter varying from 6 to 12 mm. A slightly narrower bead width (16.1 mm) was obtained at a small laser beam diameter of 4 mm due to the energy losses by vaporisation (indicated in Fig. 15). Comparing Fig. 5 and Fig. 12, one can see that the bead shape is more responsive to the total applied power than the laser beam size. It should be mentioned that the almost unchanged bead width with the variation in laser beam diameter (Fig. 12) only happens when the laser beam size is smaller than the melt pool. The fact that the melt pool with up to four-time wider width than the laser beam diameter (bead width of 16 mm at the laser beam diameter of 4 mm) was achieved suggests that the melt flow was dominant in the bead formation in these cases. However, if the beam size is bigger than the natural melt pool size, then the laser beam size would control the width. This was demonstrated by the multi-energy source (MES) approach with one leading PTA and two trailing lasers on the edges of the melt pool [9].

Fig. 13 exhibits the cross-section of the corresponding beads described in Fig. 12. It can be seen that all the penetrations on the workpiece had similar depth. Normally, the penetration depth is proportional to power density and interaction time in laser welding [21]. The power density is defined as the ratio of laser power to laser beam area which, for a circular beam, is given by:

$$E = \frac{4P_l}{\pi d_l^2} \tag{3}$$

where P_l and d_l are the laser power and laser beam diameter, respectively. The interaction time, t_i, is defined as the ratio of laser beam diameter to travel speed, which is given by:

$$t_i = \frac{d_l}{v_t} \tag{4}$$

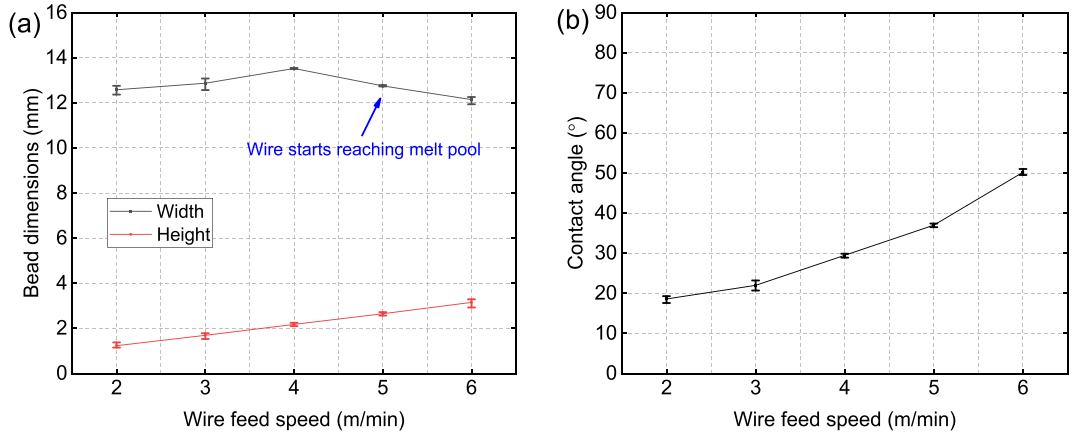

Fig. 9. The effect of WFS on (a) bead dimensions, and (b) contact angle. All the parameters used are shown in Cases (12–16) of Table 1.

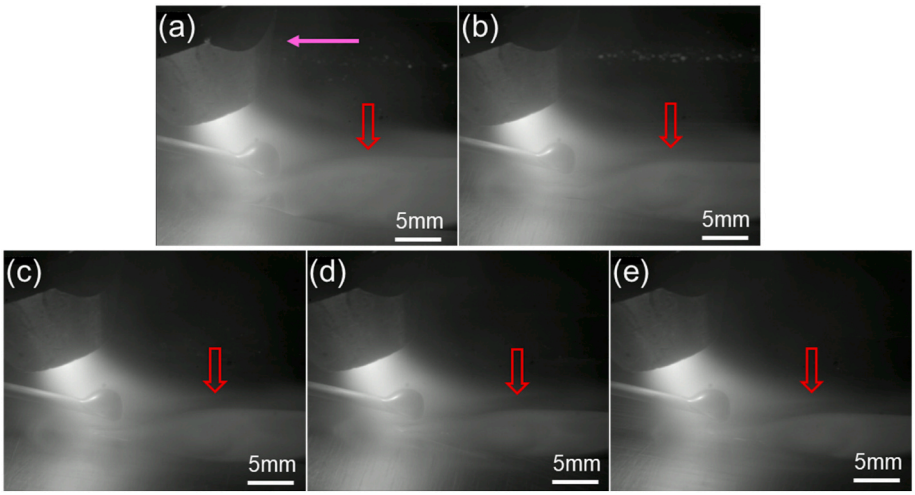

Fig. 10. Hybrid deposition processes at different TSs: (a) 4 mm/s, (b) 6 mm/s, (c) 8 mm/s, (d) 10 mm/s, and (e) 12 mm/s. Pink arrow indicates the travel direction whilst the red arrows indicate the laser positions. (For interpretation of the references to colour in this figure legend, the reader is referred to the web version of this article.)

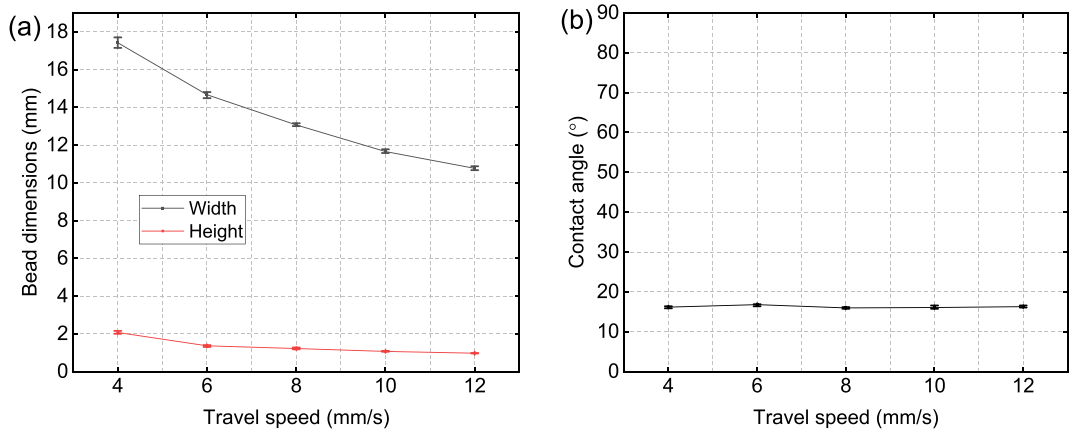

Fig. 11. The effect of TS on (a) bead dimensions, and (b) contact angle. All the parameters used are shown in Cases (17–21) of Table 1.

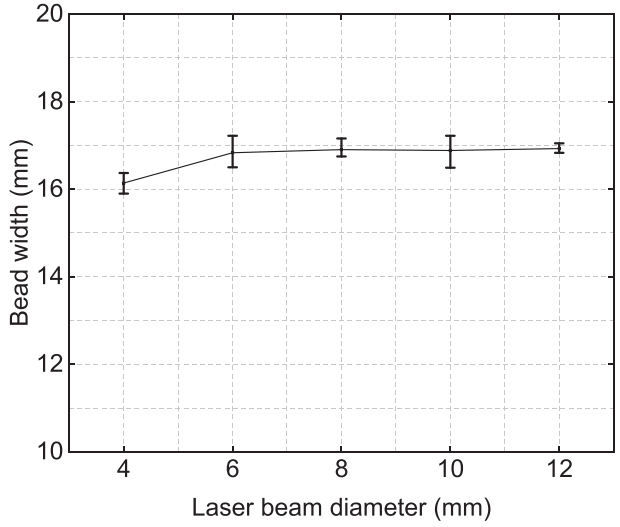

Fig. 12. The effect of laser beam size on bead width at an arc power of 4.8 kW and laser power of 5 kW. All the parameters used are shown in Cases (23–27) of Table 1.

In these cases (Fig. 12), the laser power and travel speed were fixed. Therefore, the power density reduced quadratically and the interaction time increased linearly as the laser beam diameter increased, meaning that the penetration depth should decrease as the beam diameter increases [22]. However, in this study there is PTA in front of the laser, which adds significant portion of heat to the melt pool, compensating for the deficiency of laser power and reducing the impact of laser beam size on penetration depth.

The laser power used in the cases in Figs. 12 and 13 was constant. Fig. 14 shows the effect of laser beam size on the bead width at different laser powers. It can be seen that the laser beam size had a very little effect on the bead width even at a wide range of laser power. Specifically, at the same laser power, the difference of the bead width obtained with different laser beam sizes was always less than 1 mm.

In a laser based process, the process stability is, to a large extent, dependent on the power density. Depending on the power density, there are two different regimes, known as keyhole and conduction. In general, the conduction regime exhibits still melt pool controlled by the thermal phenomena, whilst the keyhole regime is associated with vapour plume which interacts with the incoming laser beam and can induce agitated and dynamic melt pool [23]. Fig. 15 shows the PTA-laser hybrid deposition processes at different laser beam diameters and the resulting bead appearances. It can be seen that the beam diameter had a significant effect on both the process stability and bead appearance. Much smoother

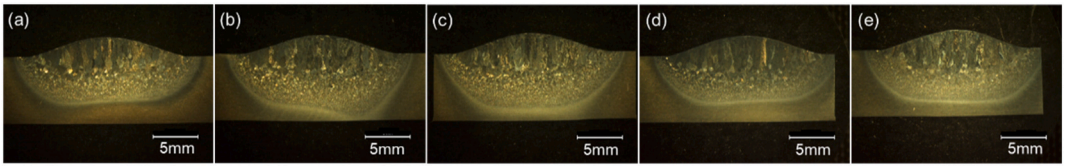

Fig. 13. The cross-section of the beads obtained with different laser beam diameters: (a) 4 mm, (b) 6 mm, (c) 8 mm, (d) 10 mm, and (e) 12 mm.

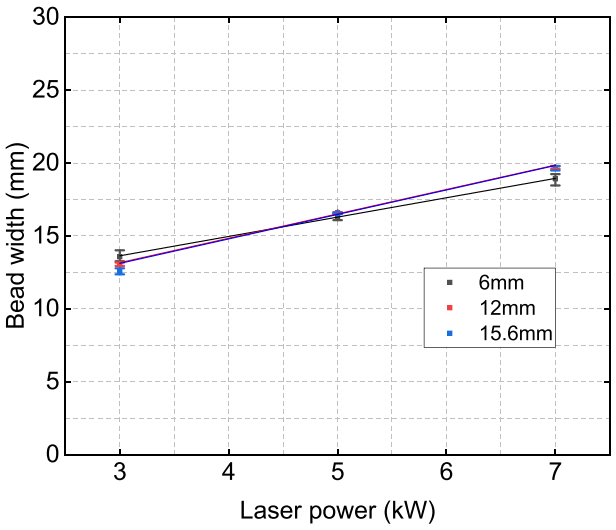

Fig. 14. The effect of laser beam size on bead width at different laser powers.

beads were achieved with larger beam diameters and therefore lower power density. When the laser beam diameter reduced to 6 mm, the onset of vaporisation occurred, evident as a bright glowing spot in the laser interaction point. This vapour plume induced random oscillation in the melt pool, resulting in a less uniform bead. Specifically, the bead obtained with the laser beam diameter of 2 mm was not straight, which is unacceptable for the deposition of parts.

3.2. Procedure for bead shape control

When depositing a high-value part, a specific bead shape and deposition rate are needed. For example, a bead shape with low contact angle is needed for near-net shape, and a relatively high deposition rate is desired for low cost and lead-time. Based on the results presented in earlier sections, a procedure for selection of different process parameters to achieve a targeted deposition rate and bead shape in the PTA-laser hybrid AM process is proposed as shown in Fig. 16, which will be introduced in detail.

For a single bead, in addition to measure the contact angle directly from the cross-sectional profile, it can also be calculated by the following equation [18]:

$$\theta = 2arctan\left(\frac{2b_h}{b_w}\right) \tag{5}$$

where b_h and b_w are bead height and head width, respectively. Therefore, when the bead dimensions are given, the cross-sectional area of the bead will be fixed. The deposition rate, R, is expressed as:

$$R = \frac{\pi d_w^2 v_w \rho}{4} \tag{6}$$

where ρ is the density of the wire, d_w is wire diameter, and v_w is WFS. Therefore, for a given wire, the deposition rate is only dependent on the WFS. From Eq. (2), one can see that when the cross-sectional area of the bead and the WFS are confirmed, the TS can be achieved. As discussed in Section 3.1.2, in the hybrid process, the PTA is used to melt the wire to take advantage of its high efficiency and arc pressure, giving smooth metal transfer. If the arc current is too low, the wire cannot be fully melted. If the current is too high, there is a large depression formed on the substrate or underlying layers, reducing the process stability (Fig. 6).

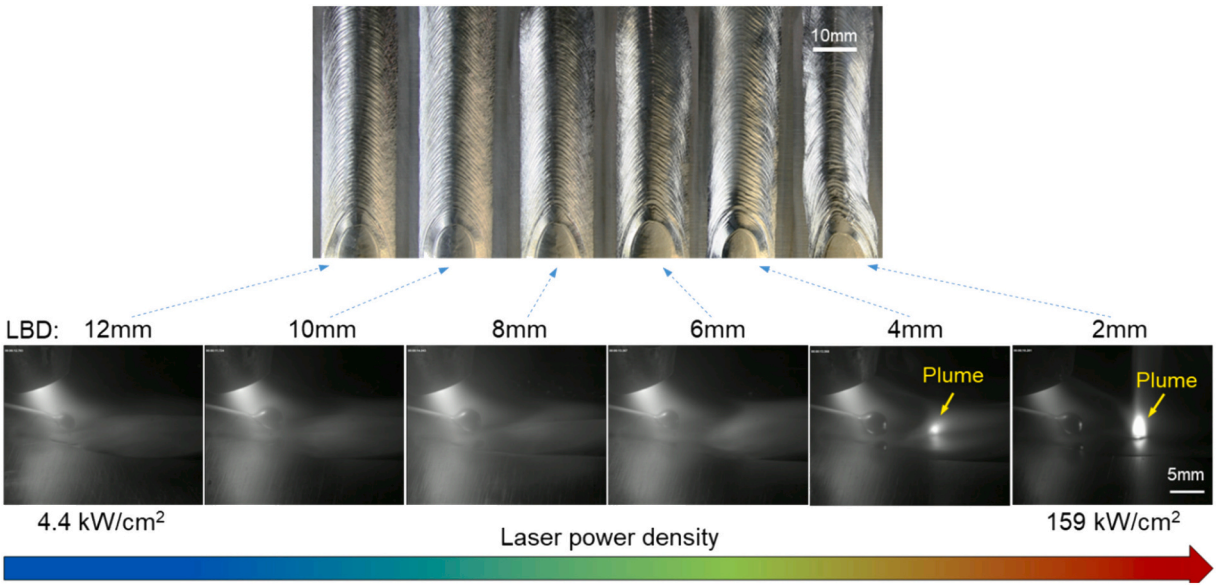

Fig. 15. The effect of laser beam size on the deposition process and bead appearance at a constant laser power of 5 kW and arc power of 4.8 kW. Note, LBD stands for laser beam diameter.

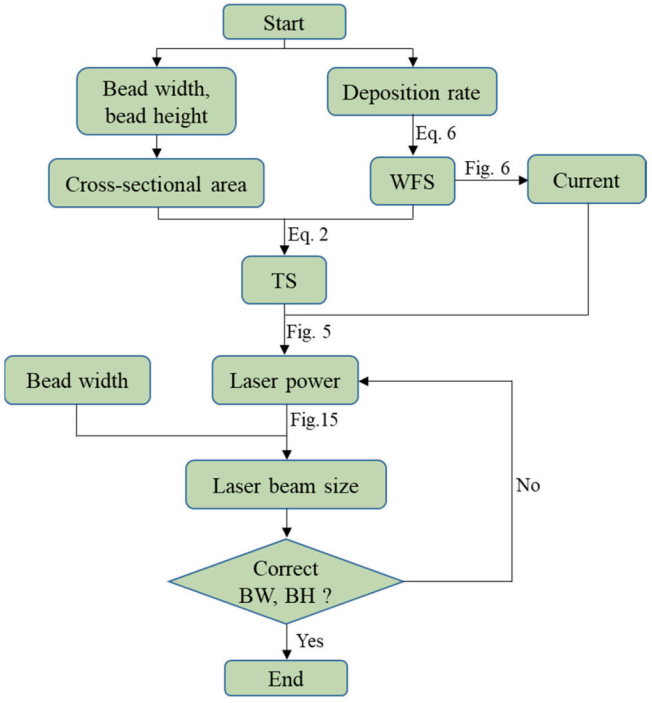

Fig. 16. Procedure for bead shape control in wire based PTA-laser hybrid AM process. Note, BW and BH stand for bead width and bead height, respectively.

Therefore, there is an optimum arc current for each given WFS. In fact, Wang et al. [20] obtained the maximum WFSs for different sizes of wires at different levels of current in the PTA deposition process, which provides a reference for the selection of arc current for the hybrid deposition process. Furthermore, the laser is used to control the melt pool size in the hybrid process. Therefore, once the WFS, TS, and current are fixed, the only way to control the bead shape is to adjust the laser power (Fig. 5). As discussed in Section 3.1.5, for a given arc power and laser power, the bead width changes very slightly with the laser beam size. However, the bead quality is largely dependent on it (Fig. 15). Therefore, to achieve a smooth and uniform bead, an optimum laser beam size should be used. In addition, when choosing the laser beam size, the bead width needs to be taken into consideration. The laser beam should not be too small to avoid low process stability and low bead quality, and it should not be much larger than the bead width to avoid excessive energy losses. After all the parameters have been confirmed, the deposited bead will be examined to check if it meets the targeted shape. If not, the laser power will be adjusted slightly until the targeted bead shape is achieved.

Overall, the hybrid deposition process should be operated in the most optimum regime with the PTA melting the feedstock wire and laser controlling the melt pool. Actually, increasing the TS does not have any effect on deposition rate or building time but mainly on the possible range of bead widths for a given process. In some cases, faster TSs are required to achieve narrow beads and maintain high deposition rates. An appropriate arc power needs to be selected to ensure the melting of the wire. The laser power should be optimum to provide just the right amount of heat for the required bead width and remelting ratio. Ideally, the laser beam size should be in the order of magnitude of the bead width to minimise the risk of vaporisation and unnecessary convective flow.

3.3. *Multi-layer single-pass walls*

To demonstrate the feasibility and repeatability of the proposed procedure, two multi-layer single-pass walls were deposited using the hybrid process. The target was to deposit two walls with the same bead dimensions (width of 12 mm and height of 1.6 mm) but different deposition rates (1.2 and 1.8 kg/h respectively). The parameters used for the two walls are listed in Table 2.

The resulting walls are shown in Fig. 17, and their properties are summarised in Table 3. It can be seen that both walls exhibit good surface finish with near-net shape, meaning such parts would require very little post-machining. The two walls have a similar profile, with small differences in layer height and width. In both cases, the real widths are slightly lower than the target. This is caused by the difference in bead dimensions between the first layer deposited on a substrate and subsequent layers [9]. Note that the parameters selected for this test were developed based on bead-on-plate experiments. In general, the achieved dimensions of the walls are very close to the target, which indicates that it is feasible to use this procedure to control the bead shape in the PTA-laser hybrid AM process.

4. Conclusions

1. The best operating regime for the PTA-laser hybrid AM process is that the wire is melted by the PTA and the melt pool is controlled by the laser. For a given WFS, the arc current is optimum when it just fully melts the wire and does not create depression or keyhole in the melt pool. Also, the laser power should be adjusted to achieve the required bead width but not too high to avoid too much remelting on the previous layers.
2. In wire based PTA-laser hybrid AM process, the bead width is affected significantly by the laser power and TS. More specifically, at a constant arc current, the bead width increases whilst the bead height decreases with increasing laser power due to the increased heat input. Both bead width and height decrease with the increase of TS, which is caused by the decreased heat input and deposited material per unit length.
3. The WFS has a relatively complex effect on the bead width. The bead width initially increases with increasing WFS and then decreases at a certain point. The increasing stage is owing to the increasing melting efficiency, whilst the decreasing stage is due to the wire reaching the melt pool, which takes a large amount of heat from the melt pool.
4. The laser beam size has very little effect on the bead shape, which suggests convection dominates the melt pool. However, it affects the process stability and the bead quality significantly. Larger beam results in a lower likelihood of vaporisation and better surface quality due to the lower power density.
5. A procedure for selecting process parameters for the achievement of required bead shape and deposition rate was proposed. Its feasibility was demonstrated by the deposition of two multi-layer single-pass walls with the same bead dimensions but different deposition rates.

Data Statement

Data underlying this study can be accessed through the Cranfield University repository at https://doi.org/10.17862/cranfield.rd.14963061.

Declaration of competing interest

The authors declare that they have no known competing financial interests or personal relationships that could have appeared to influence

Table 2
Process parameters used for deposition of two multi-layer single-pass walls.

Parameters (unit)	Wall 1	Wall 2
TS (mm/s)	4.5	6.75
WFS (m/min)	4	6
Arc current (A)	200	270
Laser beam diameter (mm)	12	12
Laser power (kW)	3	3.5

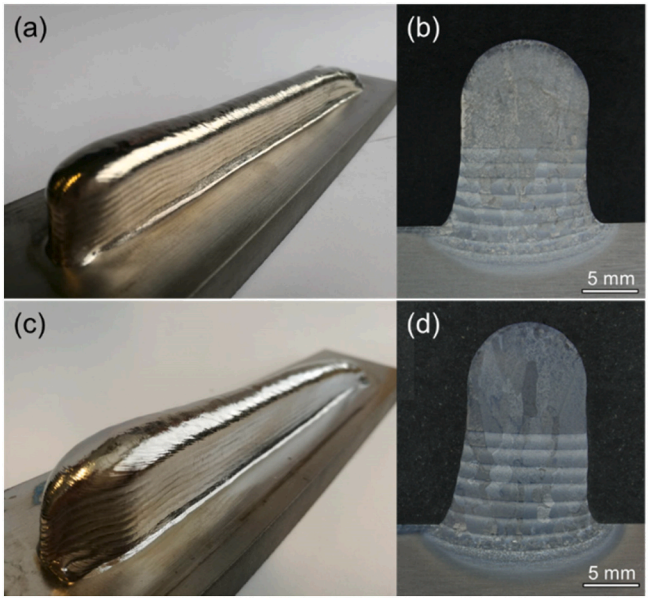

Fig. 17. Two multi-layer single-pass walls with the same bead shape but different deposition rates: (a) Wall 1 and (b) its cross-section at a deposition rate of 1.2 kg/h, and (c) Wall 2 and (d) its cross-section at a deposition rate of 1.8 kg/h.

Table 3
Features of the two multi-layer single-pass walls.

Parameters (unit)	Wall 1	Wall 2
Total layer number	10	10
Total height (mm)	17.1	18.2
Average layer height (mm)	1.7	1.8
Width (mm)	11.5	11.1
Deposition rate (kg/h)	1.2	1.8

the work reported in this paper.

Acknowledgement

Chong Wang would like to thank Welding Engineering and Laser Processing Centre (WELPC) of Cranfield University and China Scholarship Council (No. 201706450041) for funding his research studies. The authors acknowledge the funding from EPSRC (NEWAM programme: EP/R027218/1). The assistance from Dr. Jan Hönnige is much appreciated for designing the setup. The authors also would like to express their gratitude to John Thrower, Nielsen Flemming, and Nisar Shah for setting up the hybrid AM system, and Steve Pope and Tracey Roberts for etching the samples.

References

[1] DebRoy T, Wei HL, Zuback JS, Mukherjee T, Elmer JW, Milewski JO, et al. Additive manufacturing of metallic components – process, structure and properties. Prog Mater Sci 2018;92:112–224. https://doi.org/10.1016/j.pmatsci.2017.10.001.
[2] Herzog D, Seyda V, Wycisk E, Emmelmann C. Additive manufacturing of metals. Acta Mater 2016;117:371–92. https://doi.org/10.1016/j.actamat.2016.07.019.
[3] Wu B, Pan Z, Ding D, Cuiuri D, Li H, Xu J, et al. A review of the wire arc additive manufacturing of metals: properties, defects and quality improvement. J Manuf Process 2018;35:127–39. https://doi.org/10.1016/j.jmapro.2018.08.001.
[4] Williams SW, Martina F, Addison AC, Ding J, Pardal G, Colegrove P. Wire + arc additive manufacturing. Mater Sci Technol 2016;32:641–7. https://doi.org/10.1179/1743284715Y.0000000073.
[5] Qi Z, Cong B, Qi B, Sun H, Zhao G, Ding J. Microstructure and mechanical properties of double-wire + arc additively manufactured Al-cu-mg alloys. J Mater Process Technol 2018;255:347–53. https://doi.org/10.1016/j.jmatprotec.2017.12.019.
[6] Cong B, Ding J, Williams S. Effect of arc mode in cold metal transfer process on porosity of additively manufactured Al-6.3%cu alloy. Int J Adv Manuf Technol 2015;76:1593–606. https://doi.org/10.1007/s00170-014-6346-x.
[7] Wu B, Ding D, Pan Z, Cuiuri D, Li H, Han J, et al. Effects of heat accumulation on the arc characteristics and metal transfer behavior in wire arc additive manufacturing of Ti6Al4V. J Mater Process Technol 2017;250:304–12. https://doi.org/10.1016/j.jmatprotec.2017.07.037.
[8] Petrey C. Norsk titanium charts the future of flight. Modern Metals 2018. https://www.modernmetals.com/item/14713-an-additive-manufacturing-technology-undergoes-tests-and-trials-on-numerous-applications-as-it-prepares-for-takeoff.html.
[9] Wang C, Suder W, Ding J, Williams S. Wire based plasma arc and laser hybrid additive manufacture of Ti-6Al-4V. J Mater Process Technol 2021;293:1–13. https://doi.org/10.1016/j.jmatprotec.2021.117080.
[10] Shi J, Song G, Wang H, Liu L. Study on weld formation and its mechanism in laser-TIG hybrid welding with filler wire of a titanium alloy. J Laser Appl 2018;30:032004. https://doi.org/10.2351/1.5042205.
[11] Chen YB, Lei ZL, Li LQ, Wu L. Experimental study on welding characteristics of CO2 laser TIG hybrid welding process. Sci Technol Weld Join 2006;11:403–11. https://doi.org/10.1179/174329306X129535.
[12] Zhang C, Gao M, Wang D, Yin J, Zeng X. Relationship between pool characteristic and weld porosity in laser arc hybrid welding of AA6082 aluminum alloy. J Mater Process Technol 2017;240:217–22. https://doi.org/10.1016/j.jmatprotec.2016.10.001.
[13] Liu S, Liu F, Zhang H, Shi Y. Analysis of droplet transfer mode and forming process of weld bead in CO 2 laserMAG hybrid welding process. Opt Laser Technol 2012;44:1019–25. https://doi.org/10.1016/j.optlastec.2011.10.016.
[14] Chen X, Mu Z, Hu R, Liang L, Murphy AB, Pang S. A unified model for coupling mesoscopic dynamics of keyhole, metal vapor, arc plasma, and weld pool in laser-arc hybrid welding. J Manuf Process 2019;41:119–34. https://doi.org/10.1016/j.jmapro.2019.03.034.
[15] Dinovitzer M, Chen X, Laliberte J, Huang X, Frei H. Effect of wire and arc additive manufacturing (WAAM) process parameters on bead geometry and microstructure. Addit Manuf 2019;26:138–46. https://doi.org/10.1016/j.addma.2018.12.013.
[16] Martina F, Mehnen J, Williams SW, Colegrove P, Wang F. Investigation of the benefits of plasma deposition for the additive layer manufacture of Ti-6Al-4V. J Mater Process Technol 2012;212:1377–86. https://doi.org/10.1016/j.jmatprotec.2012.02.002.
[17] Schulz M, Klocke F, Riepe J, Klingbeil N, Arntz K. Process optimization of wire-based laser metal deposition of titanium. J Eng Gas Turbines Power 2019:141. https://doi.org/10.1115/1.4041167.
[18] Abioye TE, Folkes J, Clare AT. A parametric study of Inconel 625 wire laser deposition. J Mater Process Technol 2013;213:2145–51. https://doi.org/10.1016/j.jmatprotec.2013.06.007.
[19] Mok SH, Bi G, Folkes J, Pashby I. Deposition of Ti-6Al-4V using a high power diode laser and wire, part I: investigation on the process characteristics. Surf Coatings Technol 2008;202:3933–9. https://doi.org/10.1016/j.surfcoat.2008.02.008.
[20] Wang C, Suder W, Ding J, Williams S. The effect of wire size on high deposition rate wire and plasma arc additive manufacture of Ti-6Al-4V. J Mater Process Technol 2021;288:116842. https://doi.org/10.1016/j.jmatprotec.2020.116842.
[21] Ayoola WA, Suder WJ, Williams SW. Parameters controlling weld bead profile in conduction laser welding. J Mater Process Technol 2017;249:522–30. https://doi.org/10.1016/j.jmatprotec.2017.06.026.
[22] Suder W, Williams S. Parameter selection in laser welding using the power factor concept. 29th Int Congr Appl Lasers Electro-Optics, ICALEO 2010 - Congr Proc 2010;103:654–9. https://doi.org/10.2351/1.5062095.
[23] Goncalves Assuncao E. Investigation of conduction to keyhole mode transition. PhD Thesis. Cranfield University, 2012. https://dspace.lib.cranfield.ac.uk/handle/1826/7842.

2021-07-16

Bead shape control in wire based plasma arc and laser hybrid additive manufacture of Ti-6Al-4V

Wang, Chong

Elsevier

Wang C, Suder W, Ding J, Williams S. (2021) Bead shape control in wire based plasma arc and laser hybrid additive manufacture of Ti-6Al-4V. Journal of Manufacturing Processes, Volume 68, Pt.A, August 2021, pp. 1849-1859

https://doi.org/10.1016/j.jmapro.2021.07.009